Accuracy of Phase-Decoupled and Phase-Coupled Distribution Grid Power Flow Models

Adedoyin Inaolaji[◊], Alper Savasci[◊], Sumit Paudyal[◊], and Sukumar Kamalasadan[⊕]
[◊]Florida International University, USA; [⊕]University of North Carolina at Charlotte, USA
Emails: ainao003@fiu.edu, asava014@fiu.edu, spaudyal@fiu.edu, skamalas@uncc.edu

2021 IEEE Power & Energy Society Innovative Smart Grid Technologies Conference (ISGT) | 978-1-7281-8897-3/21/$31.00 ©2021 IEEE | DOI: 10.1109/ISGT49243.2021.9372193

***Abstract*—The complexity and computational burden of non-linear power flow (PF) models have motivated the introduction of various approximations. While these approximations provide tractability and reduced computational burden in PF, for optimal power flow (OPF) and control purpose, the accuracy of these models becomes a major concern in the presence of high renewable energy penetration/increased demand in distribution feeders. This paper compares and analyzes, for the first time to our knowledge, the performance of commonly used PF models in OPF formulations for single-phase and unbalanced three-phase distribution systems. Simulations performed on the phase-coupled and phase-decoupled versions of the IEEE 123-node and a reduced model extracted from the IEEE 8500-node feeder with varying levels of negative and positive net loads show that, ignoring mutual coupling impedances, as in the phase-decoupled PF models, is the largest source of error on the voltage profiles. Also, the performance of the linear PF models is acceptable only for a small range around the nominal operating point; hence, they can lead to large errors if used in OPF/control framework that seeks solutions on wider operating range.**

***Index Terms*—Distribution Grid Model, Optimal Power Flow, Linear Power Flow, Three-phase Systems.**

I. Introduction

With increasing generation diversity, evolving demand-side applications in distribution systems, and the need for real-time analyses, it has become critical to have efficient and robust power flow (PF) formulations. PF analysis is a valuable tool used by system operators for planning and operational purposes. PF models form the basic building blocks of optimization and control problems like optimal power flow (OPF) [1], unit commitment with power flow constraints [2], volt/var control [3], transmission line switching [4], etc. Thus, accurate representation of components of power systems, and the underlying laws of physics are crucial for control and optimization applications. The relationship between complex power and complex voltage renders PF equations to become non-linear and non-convex [5]. This exact PF representation is referred to as alternating current power flow (ACPF). Solving non-linear PF equations on large scale practical networks becomes computationally costly as the network size increases, particularly in applications requiring multiple runs of PF (e.g, hosting capacity analysis [6]) or in OPF. Hence, there is a tradeoff between accuracy and computational burden when using the exact ACPF models. Moreover, in an OPF framework, the non-convex feasible space of the non-linear PF equations can lead to local solutions. Therefore, developing novel and efficient PF formulations continues to be an active area of research. Approximate and linearized models of power flow equations have been widely proposed in the literature. Approximations provide tractable formulations that represent power flow physics by making assumptions about certain system behavior and characteristics [7].

In the seminal work [8], [9], a recursive non-linear branch flow model (BFM), called *DistFlow*, is introduced. *DistFlow* models PF in terms of the branch power, current, and bus voltages, while neglecting voltage and current angles. As *DistFlow* provides reasonably accurate PF solutions, the model has been extensively used in convex version of OPF by reformulating branch flow constraints as second order cone [10]. The non-linear *DistFlow* model is linearized by eliminating loss components to obtain *LinDistFlow*, which is applied for optimal capacitor sizing and placement in radial networks in [8], [9], and for reactive power control in [11]. In [12], *LinDistFlow* is further simplified and the resulting linear model is used in a local control scheme to optimize the reactive power dispatch of photovoltaic (PV) inverters in a distribution network. Note that the models in [8]–[11] are expressed in terms of square of the voltage magnitudes. In [13], complex voltage is represented in rectangular coordinates and an approximate linear model is derived by eliminating quadratic terms in the non-linear PF equations. This linear model is applied to an OPF problem in distribution networks for inverter dispatch [14]. The formulations in [8], [12], [14] are applied for single-phase systems. However, these formulations could be applied to phase-decoupled multi-phase circuits, where the multi-phase circuits are decoupled into single-phase circuits by ignoring the mutual coupling of phases as in [15].

Distribution systems, however, require consideration of unbalanced operation and multi-phase structure with the inclusion of mutual coupling. In this context, [16] extends *LinDistFlow* to unbalanced multi-phase networks, resulting in a new model called *LinDist3Flow*. *LinDist3Flow* assumes that the ratio of phase voltage magnitudes is constant, phase angles of the three phases are equally spaced, and losses are ignored. The accuracy of the model is tested within an

This work is supported by the U.S. Department of Energy's Office of Energy Efficiency and Renewable Energy (EERE) under the Solar Energy Technologies Office Award Number DE-EE0008774. Corresponding Author: Adedoyin Inaolaji, Email: ainao003@fiu.edu.

optimization model and compared with a convex relaxation. However, no information is provided about the accuracy of the *LinDist3Flow* solution compared to the exact power flow solution.

The existing linear models [8], [9], [12], [14], [16] are good approximations of the original non-linear models around an operating point. With increasing renewable energy penetration and for higher loading conditions, the accuracy of these models becomes a concern. Therefore, in OPF or other control applications that seek for the (optimal) operating point in a wider operating range (e.g., the permissible voltage between 0.95-1.05 p.u.), these models may exhibit larger errors, which could lead to sub-optimal (or even infeasible) economic and technical decisions by utilities. Thus, users need to be careful when selecting the operational range for which the models in [8], [9], [12], [14], [16] are sufficiently accurate. In this context, this paper revisits various approximate PF models and provides valuable information to the users about the accuracy of the models, and operating ranges for which the models are best suited for. We compare and analyze, for the first time to our knowledge, the performance of commonly used PF models in OPF formulations for single-phase and unbalanced three-phase distribution systems.

The rest of this paper is organized as follows. Section II provides the mathematical formulations of power flow models most commonly used in literature. Section III presents case studies to analyze the performance of the models. The paper is concluded in Section IV.

II. Power Flow Models

A distribution network is represented by a set of $\mathcal{B}$ buses, and a set of $\mathcal{L}$ lines connecting these buses. The index of the buses are denoted by *i= 0,1,2,...,n*, where *n* is the total number buses in the network, and $\mathcal{B}' = \mathcal{B}\backslash\{0\}$. j is defined as an alias of i. Bus 0 is slack bus, representing the substation node with voltage fixed to the nominal value. Let u_i^ϕ denote the phase ϕ complex voltage at bus i, and $U_i^\phi = \left|u_i^\phi\right|^2$. Let $\mathbf{v}_i = \left[u_i^a, u_i^b, u_i^c\right]^T$ denote the vector of complex voltages at bus i, and $\mathbb{V}_i = \mathbf{v}_i\mathbf{v}_i^*$. $z_{ij}^{\phi\phi} = r_{ij}^{\phi\phi} + \mathbf{j}x_{ij}^{\phi\phi}$ denotes the self impedance of line $(i,j) \in \mathcal{L}$ and $z_{ij}^{\phi\beta} = r_{ij}^{\phi\beta} + \mathbf{j}x_{ij}^{\phi\beta}$, for $\phi \neq \beta$, denotes the mutual impedance of the line, where β is defined as an alias of ϕ. $\mathbb{Z}_{ij}$ denotes the three-phase impedance of the line. Let I_j^ϕ denote the complex phase ϕ current flowing on line (i,j) into bus j and $\ell_j^\phi = \left|I_j^\phi\right|^2$. Let $\mathbf{m}_j = \left[I_j^a, I_j^b, I_j^c\right]^T$ denote the vector of complex currents and let $\mathbb{M}_j = \mathbf{m}_j\mathbf{m}_j^*$. Let $S_j^\phi = P_j^\phi + \mathbf{j}Q_j^\phi$ be the phase ϕ sending-end complex power flowing out of bus i towards bus j. $\mathbf{S}_j = \left[S_j^a, S_j^b, S_j^c\right]^T$ denotes the vector of complex power. $s_i^\phi = p_i^\phi + \mathbf{j}q_i^\phi$ is the phase ϕ complex net power injection at node i, and $\mathbf{s}_i = \left[s_i^a, s_i^b, s_i^c\right]^T$ is the vector of complex power phasors injected into bus i. $\mathbf{i}_i^\phi$ is the phase current injected into bus i. $\mathbf{i}_n^\phi$ and u_n^ϕ denote the current injections and voltages respectively at $\mathcal{B}'$.

A. Phase-Decoupled Power Flow Models

The phase-decoupled model (equivalent to single phase) using BFM approach can represented by the following set of equations [10].

$$u_i^\phi - u_j^\phi = z_{ij}^{\phi\phi} I_j^\phi \tag{1}$$

$$S_j^\phi = u_i^\phi I_j^{\phi *} \tag{2}$$

$$s_j^\phi = \sum_{k:j\to k} S_k^\phi - \left(S_j^\phi - z_{ij}^{\phi\phi}\left|I_j^\phi\right|^2\right) \tag{3}$$

Equations (1)-(3), hereafter referred to as *AC1PF*, represents exact non-linear model.

By substitution and decomposition of *AC1PF* into real and imaginary parts, *DistFlow* equations are obtained as in (4)-(7) [10].

$$p_j^\phi = \sum_{k:j\to k} P_k^\phi - \left(P_j^\phi - r_{ij}^{\phi\phi}\ell_j^\phi\right) \tag{4}$$

$$q_j^\phi = \sum_{k:j\to k} Q_k^\phi - \left(Q_j^\phi - x_{ij}^{\phi\phi}\ell_j^\phi\right) \tag{5}$$

$$U_j^\phi = U_i^\phi - 2\left(r_{ij}^{\phi\phi}P_j^\phi + x_{ij}^{\phi\phi}Q_j^\phi\right) + \left(r_{ij}^{\phi\phi 2} + x_{ij}^{\phi\phi 2}\right)\ell_j^\phi \tag{6}$$

$$\ell_j^\phi = \frac{P_j^{\phi 2} + Q_j^{\phi 2}}{U_i^\phi} \tag{7}$$

Although the voltage and current angles are dropped in the *DistFlow* equations, it yields similar results as the *AC1PF* model. Moreover, the angles can be recovered using the angle recovery algorithm as in [10].

Equation (7) renders the *DistFlow* non-linear. To overcome the complexity of non-linearity, the losses are ignored and current magnitude terms are eliminated to obtain the *LinDistFlow* model (8)-(10).

$$p_j^\phi = \sum_{k:j\to k} P_k^\phi - (P_j^\phi) \tag{8}$$

$$q_j^\phi = \sum_{k:j\to k} Q_k^\phi - (Q_j^\phi) \tag{9}$$

$$U_j^\phi = U_i^\phi - 2\left(r_{ij}^{\phi\phi}P_j^\phi + x_{ij}^{\phi\phi}Q_j^\phi\right) \tag{10}$$

In [12], U_j is approximated as $U_0 + 2u_0\left(u_j - u_0\right)$ and (10) becomes,

$$u_j^\phi = u_i^\phi - \left(r_{ij}^{\phi\phi}P_j^\phi + x_{ij}^{\phi\phi}Q_j^\phi\right)/u_0^\phi \tag{11}$$

Equations (8), (9), and (11) are hereafter called *LinDistSimp* model.

Using the bus injection model and given the bus admittance matrix Y, the nodal current and power injection are given by,

$$\begin{bmatrix}\mathbf{i}_0^\phi \\ \mathbf{i}_n^\phi\end{bmatrix} = \begin{bmatrix}Y_{ss} & Y_{sn} \\ Y_{ns} & Y_{nn}\end{bmatrix}\begin{bmatrix}u_0^\phi \\ u_n^\phi\end{bmatrix} \tag{12}$$

$$s_i^\phi = u_i^\phi I_i^{\phi *}, \quad \forall i \in \mathcal{B} \tag{13}$$

Given that $Y_{nn}^{-1} = R + \mathrm{j}X$, [14] linearizes (13) by expressing $u_n^\phi = u_0^\phi + \Delta u$. In rectangular coordinates, the nodal voltage is expressed as,

$$\mathbf{Re}\left\{u_i^\phi\right\} = u_0^\phi + \sum_{j\in\mathcal{B}'}\left(R_{ij}p_j^\phi + X_{ij}q_j^\phi\right) \quad \forall i \in \mathcal{B}' \tag{14}$$

$$\mathbf{Im}\left\{u_i^\phi\right\} = \sum_{j\in\mathcal{B}'}\left(X_{ij}p_j^\phi - R_{ij}q_j^\phi\right). \quad \forall i \in \mathcal{B}' \tag{15}$$

Equations (14), (15) are hereafter called *LinDistRC* model.

B. Phase-Coupled Power Flow Models

In a three-phase network, the power flow is modelled by the following set of BFM equations [17],

$$\mathbf{v}_i - \mathbf{v}_j = \mathbb{Z}_{ij}\mathbf{m}_j \tag{16}$$

$$\mathbf{S}_j = \mathbf{v}_i\,\mathbf{m}_j^* \tag{17}$$

$$\sum_{k:j\to k} \mathrm{diag}\,\mathbf{S}_k - \mathrm{diag}\left(\mathbf{S}_j - \mathbb{Z}_{ij}\mathbb{M}_j\right) = \mathbf{s}_j \tag{18}$$

Equations (16)-(18), hereafter referred to as *AC3PF*, represent a non-linear model and it includes the mutual coupling among the phases. Hence, it is an exact representation.

In [16], the ratio of voltage phasors is approximated by constants as,

$$u_i^a(u_i^b)^{-1} \approx \alpha \quad u_i^b(u_i^c)^{-1} \approx \alpha \quad u_i^a(u_i^c)^{-1} \approx \alpha^2 \tag{19}$$

where $\alpha = 1\angle 120° = \frac{-1+\mathrm{j}\sqrt{3}}{2}$, $\alpha^2 = 1\angle 240° = -\frac{1+\mathrm{j}\sqrt{3}}{2}$

Loss terms are ignored in (18) to obtain

$$\sum_{k:j\to k}\mathbf{S}_k - \sum_{i:i\to j}\mathbf{S}_j = \mathbf{s}_j, \tag{20}$$

The following linear model is therefore derived,

$$\mathbb{V}_i = \mathbb{V}_j - \mathbb{H}_{ij}^P\mathbf{P}_j - \mathbb{H}_{ij}^Q\mathbf{Q}_j \tag{21}$$

where,

$$\mathbb{H}_{ij}^P = \begin{bmatrix} -2r_{ij}^{aa} & r_{ij}^{ab} - \sqrt{3}x_{ij}^{ab} & r_{ij}^{ac} + \sqrt{3}x_{ij}^{ac} \\ r_{ij}^{ba} + \sqrt{3}x_{ij}^{ba} & -2r_{ij}^{bb} & r_{ij}^{bc} - \sqrt{3}x_{ij}^{bc} \\ r_{ij}^{ca} - \sqrt{3}x_{ij}^{ca} & r_{ij}^{cb} + \sqrt{3}x_{ij}^{cb} & -2r_{ij}^{cc} \end{bmatrix} \tag{22}$$

$$\mathbb{H}_{ij}^Q = \begin{bmatrix} -2x_{ij}^{aa} & x_{ij}^{ab} + \sqrt{3}r_{ij}^{ab} & x_{ij}^{ac} - \sqrt{3}r_{ij}^{ac} \\ x_{ij}^{ba} - \sqrt{3}r_{ij}^{ba} & -2x_{ij}^{bb} & x_{bc} + \sqrt{3}r_{ij}^{bc} \\ x_{ij}^{ca} + \sqrt{3}r_{ij}^{ca} & x_{ij}^{cb} - \sqrt{3}r_{ij}^{cb} & -2x_{ij}^{cc} \end{bmatrix} \tag{23}$$

The *LinDist3Flow* is modelled by (20)-(23) [16].

III. Performance Analysis

To analyze the performance of the PF models described in Section II, we present case studies performed on the phase-decoupled and phase-coupled circuits of the IEEE 123-node and a 650-node network (extracted from the IEEE 8500-node network) [18]. For phase-decoupled analyses, we decouple the networks into three single phases similar to the approach used in [15]. Bus 0 is a slack bus and is fixed to nominal voltage value. Voltage regulators are disabled and switches are modelled as open/shorted lines depending on their status. Distributed loads are ignored and all spot loads are modelled as constant power loads with wye connection. Line shunt parameters are ignored and capacitor banks are modelled as constant reactive power source.

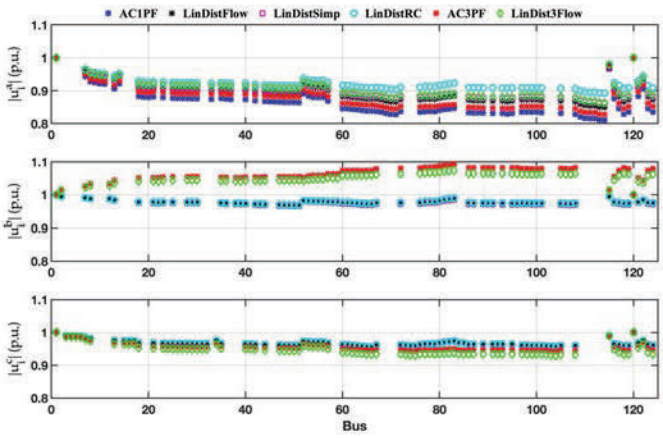

Fig. 1. Voltage profiles on the 123-node feeder for unbalanced base load.

A. Phase-Decoupled vs. Phase-Coupled Models

First, we compare the performance of six PF models described in Section II. We exclude *DistFlow* from comparison as solutions from *DistFlow* and *AC1PF* models are very close [10]. Fig. 1 and Fig. 2 show the voltage profile for unbalanced loading with base load (3.49 MW) and light load (0.1 MW) conditions, respectively, on the IEEE 123-node system. The loads are highly unbalanced with 76%, 11% and 13% of total loads on phase-a, b, and c respectively. Note that *AC3PF* is the phase-coupled exact model for three-phase systems. Fig. 1 shows that in three-phase systems, the *LinDist3Flow* is the best linear approximation model of *AC3PF* compared to the other PF models as *LinDist3Flow* considers mutual coupling of phases. Performance of *AC1PF*, *LinDistFlow*, *LinDistSimp*, and *LinDistRC* show large errors compared to *AC3PF* as these methods ignore mutual coupling in three-phase systems. Fig. 2 shows that for light load, the errors decrease with respect to *AC3PF* for all models; still, phase-decoupled linear models consistently exhibit larger errors compared to the phase-coupled model. Based on Figs. 1 and 2, we cannot conclude whether a particular model is an under-estimator or over-estimator with respect to the exact solution from *AC3PF* for phase-coupled systems, as this is more dependent on the interaction of phase coupling and loads in each phase. Thus, these methods perform very differently on each phase and with different loading scenario.

Fig. 3a shows the root mean square error (RMSE) on voltage with respect to *AC3PF* at different levels of positive and negative net loads on the 123-node. Positive net load indicates that load is greater than the aggregated renewable generation, while negative net load indicates that renewable generation is greater than load. A net load of 0% is equivalent to no-load condition; however, fixed reactive power from capacitor banks are included for all loading levels. As intuitively expected, all the models yield the most accurate results at zero net load conditions, while the error increases with positive/negative net load. When the cap banks are disabled, all the models yield zero error at 0% net load condition, which is trivial (not

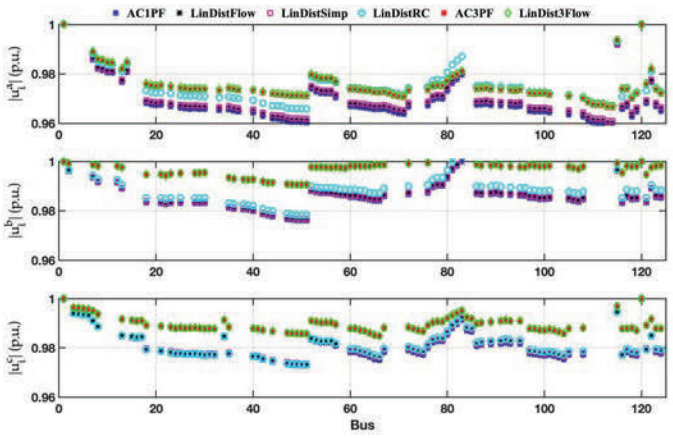

Fig. 2. Voltage profiles on the 123-node feeder for unbalanced light load.

shown in the figure). For all net load conditions, *LinDist3Flow* exhibits the smallest RMSE. Note that the phase-decoupled models (*AC1PF*, *LinDistFlow*, *LinDistSimp*, and *LinDistRC*) show similar RMSE performance for the entire range of net load considered. The RMSE of the phase-decoupled models stays around 0.07 p.u. for base load condition, while the RMSE of the phase-coupled model (*LinDist3Flow*) is just above 0.02 p.u. This demonstrates the effect of ignoring phase coupling on the voltage profile of three-phase systems.

For large-scale considerations, we also examined the performance of these PF models on a large network. The IEEE 8500-node feeder is reduced to a 650-node feeder by eliminating the load transformers and triplex lines and aggregating the loads upstream on the three-phase buses which are on the medium voltage side. A total real power load of about 11 MW is evenly distributed across the phases. As shown in Fig. 3b, the RMSE from linear phase-decoupled methods (*LinDistFlow*, *LinDistSimp*, and *LinDistRC*) become larger with increase in size of the network.

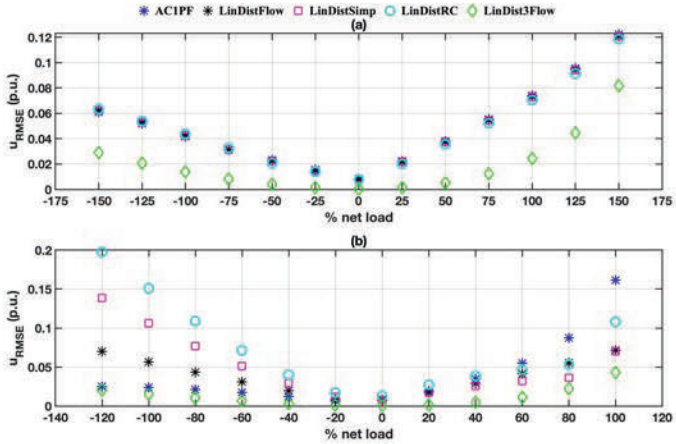

Fig. 3. RMSE on nodal voltages from different PF models compared to *AC3PF* on (a) 123-node and, (b) 650-node systems.

B. Analysis of Phase-Decoupled Models

Most of the linear grid models used in OPF formulations are phase-decoupled, which is equivalent to solving three single-phase systems. Thus, it would be meaningful to compare the performance of phase-decoupled models with respect to a single-phase exact non-linear model. Note that the *DistFlow* model, which is non-linear, provides an accurate solution compared to the exact single-phase *AC1PF* model, thus it is not included in the analysis. Fig. 4a compares the RMSE of *LinDistFlow*, *LinDistSimp*, and *LinDistRC* with respect to *AC1PF* on the phase-decoupled circuits of the IEEE 123-node test feeder. It shows that the *LinDistFlow* exhibits the least error, while *LinDistRC* has the highest error blue in a wide range of load penetration levels : does this portray pv penetration. At nominal loading condition, *LinDistRC* has RMSE of about 0.05 p.u. on voltage. Fig. 4b shows a similar comparison on the 650-node feeder. Results are consistent on both feeders that the *LinDistRC* exhibits largest RMSE, followed by *LinDistSimp* and *LinDistFlow*. Therefore, for single-phase, analysis, *LinDistFlow* is the most accurate linear model among the three linear models considered.

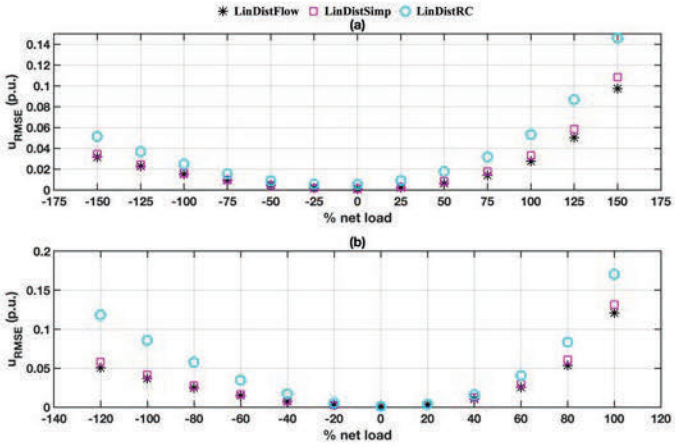

Fig. 4. RMSE on nodal voltages from different phase-decoupled PF models compared to *AC1PF* on (a) 123-node and, (b) 650-node systems.

C. Analysis of Phase-Coupled Models

In Section III.A, we showed that the *LinDist3Flow* model exhibits the least RMSE compared to the exact non-linear phase-coupled *AC3PF* model as *LinDist3Flow* model does not drop the mutual impedances. However, the assumptions made on the derivation of *LinDist3Flow* certainly requires error evaluation at different loading and unbalanced conditions. To examine this, case studies are run on the IEEE 123-node using the same total base load (3.94 MW) as in the case study in Section III.A, but the loads are evenly distributed among the phases to create a balanced loading scenario. Compared to the voltage profile of *LinDist3Flow* in Fig. 1 for unbalanced case, the voltage profile for the balanced case in Fig. 5 shows less error compared to the corresponding *AC3PF* results. The RMSE for a balanced loading condition is 0.0017 p.u. compared to the RMSE of 0.024 p.u. for unbalanced loading for the same total load.

When we repeated the simulation for the light load (0.1 MW) with a balanced and unbalanced loading condition on

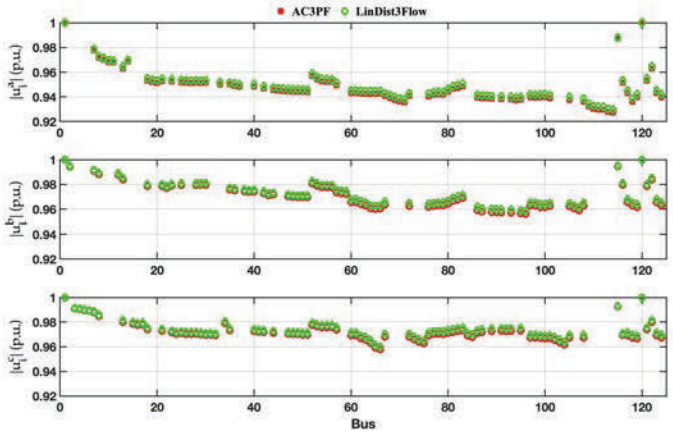

Fig. 5. Comparison of voltage profile obtained from *AC3PF* and *LinDist3Flow* for a balanced base load on the IEEE 123-node feeder.

the IEEE 123-node test feeder, we observed that the impact of unbalancing is less. Fig. 6 shows the voltage profile for the light load with a balanced loading condition obtained from the *LinDist3Flow*, which is fairly close to the solutions obtained from *AC3PF*. This is very close to the voltage profiles obtained in Fig. 2 for the light load with the unbalanced condition. The RMSE is close to 0.0004 p.u for both balanced and unbalanced loading conditions. Case studies show that the net load level and load unbalancing both impacts on the accuracy of the *AC3PF*; however, the effect of phase unbalancing is pronounced for the higher net load.

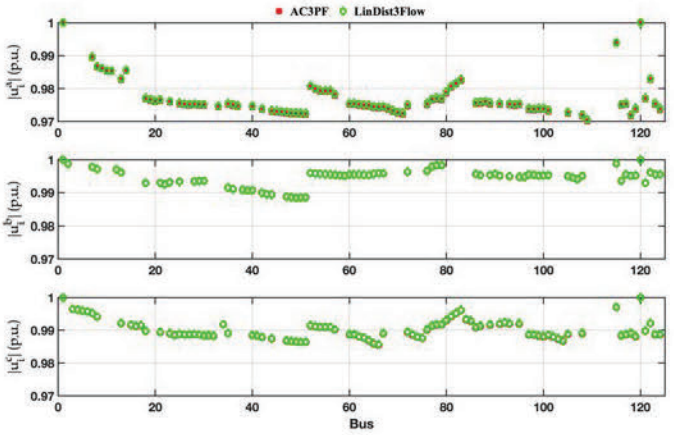

Fig. 6. Comparison of voltage profile obtained from *AC3PF* and *LinDist3Flow* for a balanced light load on the IEEE 123-node feeder.

IV. Conclusion

In this paper, we analyzed the performance of commonly used phase-decoupled and phase-coupled models of power flow. Based on the simulation results carried out on the IEEE 123-node feeder and a 650-node system, we observed that the phase-decoupled models exhibit the largest error as the mutual impedance of the lines are dropped on these models. For single-phase equivalent analysis, the results show that the *LinDistFlow* provides the most accurate solution of the nodal voltages. Among all the linear models examined, *LinDist3Flow* exhibits the least error as the mutual couplings are included in the model. The case studies demonstrated that all the linear models perform reasonably well for a small range around normal operating point; however, these linear models should be carefully considered if the objective is to solve OPF in a broader operating range.

References

[1] S. Paudyal, C. A. Canizares, and K. Bhattacharya, "Optimal operation of distribution feeders in smart grids," *IEEE Transactions on Industrial Electronics*, vol. 58, no. 10, pp. 4495–4503, 2011.

[2] A. Savasci,, A. Inaolaji, and S. Paudyal, "Performance analysis of mixed-integer conic and mixed-integer linear unit commitment models," in *Proc. IEEE Power Energy Society General Meeting (PESGM)*, 2020, pp. 1–5.

[3] M. Farivar, C. R. Clarke, S. H. Low, and K. M. Chandy, "Inverter VAR control for distribution systems with renewables," in *Proc. IEEE international conference on smart grid communications (SmartGridComm)*, 2011, pp. 457–462.

[4] B. Kocuk, S. S. Dey, and X. A. Sun, "New formulation and strong MISOCP relaxations for AC optimal transmission switching problem," *IEEE Transactions on Power Systems*, vol. 32, no. 6, pp. 4161–4170, 2017.

[5] D. Bienstock and A. Verma, "Strong NP-hardness of AC power flows feasibility," *arXiv preprint arXiv:1512.07315*, 2015.

[6] A. Dubey, S. Santoso, and A. Maitra, "Understanding photovoltaic hosting capacity of distribution circuits," in *Proc. IEEE Power Energy Society General Meeting*, 2015, pp. 1–5.

[7] D. K. Molzahn and I. A. Hiskens, *A survey of relaxations and approximations of the power flow equations*. Now Publishers, 2019.

[8] M. Baran and F. F. Wu, "Optimal sizing of capacitors placed on a radial distribution system," *IEEE Transactions on Power Delivery*, vol. 4, no. 1, pp. 735–743, 1989.

[9] M. E. Baran and F. F. Wu, "Optimal capacitor placement on radial distribution systems," *IEEE Transactions on power Delivery*, vol. 4, no. 1, pp. 725–734, 1989.

[10] M. Farivar and S. H. Low, "Branch flow model: Relaxations and convexification—Part I," *IEEE Transactions on Power Systems*, vol. 28, no. 3, pp. 2554–2564, 2013.

[11] S. Magnússon, G. Qu, and N. Li, "Distributed optimal voltage control with asynchronous and delayed communication," *IEEE Transactions on Smart Grid*, vol. 11, no. 4, pp. 3469–3482, 2020.

[12] K. Turitsyn, P. Sulc, S. Backhaus, and M. Chertkov, "Local control of reactive power by distributed photovoltaic generators," in *Proc. First IEEE International Conference on Smart Grid Communications*, 2010, pp. 79–84.

[13] S. V. Dhople, S. S. Guggilam, and Y. C. Chen, "Linear approximations to AC power flow in rectangular coordinates," in *Proc. 53rd Annual Allerton Conference on Communication, Control, and Computing (Allerton)*, 2015, pp. 211–217.

[14] S. S. Guggilam, E. Dall'Anese, Y. C. Chen, S. V. Dhople, and G. B. Giannakis, "Scalable optimization methods for distribution networks with high PV integration," *IEEE Transactions on Smart Grid*, vol. 7, no. 4, pp. 2061–2070, 2016.

[15] L. Gan, N. Li, U. Topcu, and S. H. Low, "Exact convex relaxation of optimal power flow in radial networks," *IEEE Transactions on Automatic Control*, vol. 60, no. 1, pp. 72–87, 2014.

[16] M. D. Sankur, R. Dobbe, E. Stewart, D. S. Callaway, and D. B. Arnold, "A linearized power flow model for optimization in unbalanced distribution systems," *arXiv preprint arXiv:1606.04492*, 2016.

[17] L. Gan and S. H. Low, "Convex relaxations and linear approximation for optimal power flow in multiphase radial networks," in *Proc. Power Systems Computation Conference*, 2014, pp. 1–9.

[18] K. P. Schneider, B. A. Mather, B. C. Pal, C. . Ten, G. J. Shirek, H. Zhu, J. C. Fuller, J. L. R. Pereira, L. F. Ochoa, L. R. de Araujo, R. C. Dugan, S. Matthias, S. Paudyal, T. E. McDermott, and W. Kersting, "Analytic considerations and design basis for the ieee distribution test feeders," *IEEE Transactions on Power Systems*, vol. 33, no. 3, pp. 3181–3188, 2018.